

Distinguishing characteristics of stem cells derived from different anatomical regions of human degenerated intervertebral discs

Hai Wang^{1,2} · Yue Zhou¹ · Tong-Wei Chu¹ · Chang-Qing Li¹ · Jian Wang¹ · Zheng-Feng Zhang¹ · Bo Huang¹

Received: 9 January 2015 / Revised: 5 March 2016 / Accepted: 6 March 2016 / Published online: 16 March 2016
© Springer-Verlag Berlin Heidelberg 2016

Abstract

Introduction Several types of stem cells have been successfully demonstrated to exist in the human degenerated intervertebral disc (IVD), which is composed of annulus fibrosus (AF), nucleus pulposus (NP) and cartilage endplate (CEP). However, the differences in the biological characteristics among these and bone marrow derived mesenchymal stem cells (BM-MSCs) remain unclear.

Materials and methods To investigate this issue, cells were harvested from human AF, NP, CEP, and bone marrow, respectively; passage 2 cells were selected using the agarose suspension culture system to obtain stem cell clones. Following expansion in vitro, stem cells from different anatomical regions were compared regarding the morphology, proliferation ability, immunophenotypic expression, and multi-lineage differentiation capacity. In addition, stem cell-alginate bead compositions were constructed for the comparison of DNA and sGAG content.

Results There were subtle differences regarding cell morphology, but no significant differences in proliferation ability among the four types of stem cells. For the immunophenotypic analysis, all stem cells basically fulfilled the criteria for mesenchymal stem cells (MSCs), which have been published by the International Society for Cellular Therapy (ISCT), with a significant difference in

CD105 expression. A comparison of the osteogenic capacities indicated: cartilage endplate-derived stem cells (CESCs) > annulus fibrosus-derived stem cells (AFSCs) > BM-MSCs > nucleus pulposus-derived stem cells (NPSCs). The chondrogenesis difference was similar to osteogenesis. For adipogenesis: BM-MSCs > NPSCs > CESCs > AFSCs. In the stem cell/alginate composition, the CESCs consistently showed the superior chondrogenic potential among all those cell types. **Conclusions** Our data indicated that all the four types of stem cells shared some similar biological properties (regarding shape, proliferation ability and immunophenotypic expression). CESCs, which had the strongest osteogenic and chondrogenic potentials, may serve as excellent seed cells for NP/cartilage or bone tissue engineering.

Keywords Tissue-specific stem cells · Comparison · Intervertebral disc · Biological characteristics

Introduction

An IVD is an adjacent cartilaginous joint that connects two adjacent vertebrae and absorbs the shock of the body [1]. In general views of anatomy, an IVD is an avascular organ composed of three major tissue components: AF, NP and CEP [1]. AF consists of several annular layers of elastic fiber and fibrocartilage, and it is divided into the outer AF and inner AF layers (Fig. 1) [2]. The outer layer is primarily composed of type II collagen, whereas the inner layer is primarily composed of type I collagen [3]. NP is a gelatinous matrix comprised of abundant proteoglycan and collagen fibril, which primarily comprises an abundance of collagen II [4]. Combined with AF, the NP construction provides IVD with resistance against overload by attracting

✉ Bo Huang
bighuang2000@hotmail.com

¹ Department of Orthopaedics, Xinqiao Hospital, Third Military Medical University, Chongqing 400037, People's Republic of China

² Department of Orthopaedics, Kunming General Hospital of Chengdu Military Command, Kunming 650032, People's Republic of China

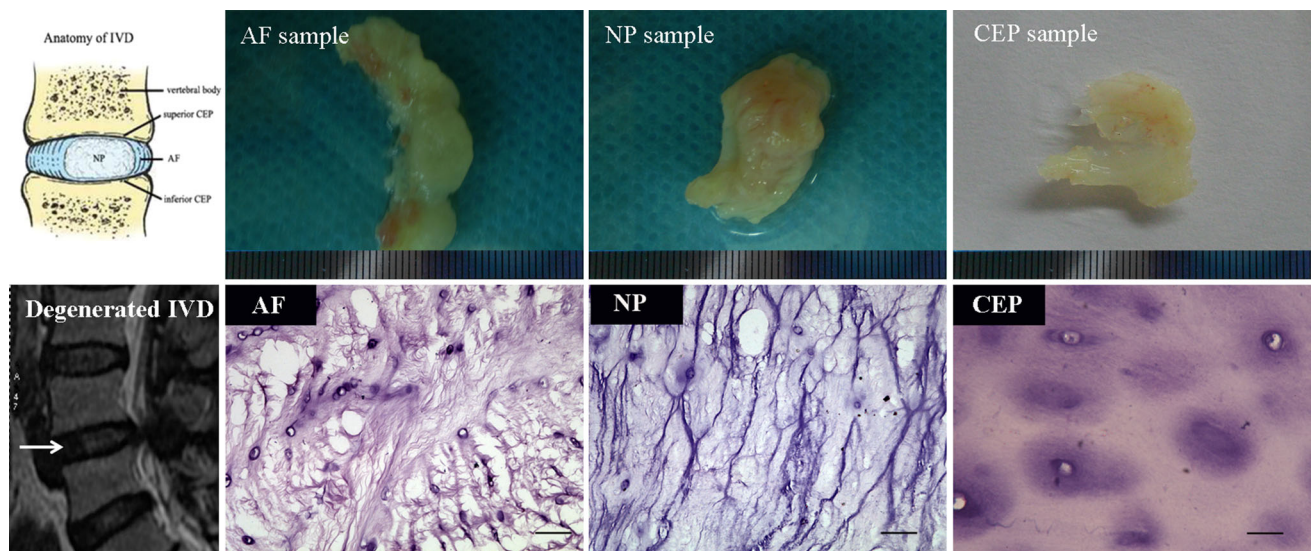


Fig. 1 IVD comprises AF, NP and CEP in anatomy. The samples were obtained from the human degenerated IVD approved in MRI. Different anatomical parts were verified by H&E staining. *White*

arrow indicates the degenerated IVD. *IVD* intervertebral disc, *AF* annulus fibrosus, *NP* nucleus pulposus, *CEP* cartilage endplate (*Bar* 100 μ m)

water [5]. CEP comprises two thin layers of hyaline cartilage on the superior and inferior surfaces of IVD, which sandwiches AF and NP [6]. From an anatomical viewpoint, NP is located in the center of an IVD and is enclosed by AF and CEP [7]. Different anatomical components perform their respective duties to maintain normal IVD function and participate in the IVD degenerative process via biomechanical and metabolic approaches (Fig. 1) [8, 9].

In recent years, mesoderm-derived MSCs have been successively isolated from nearly all types of tissues, such as peripheral blood, cord blood, trabecular bone, adipose tissue, synovium, muscle, and brain [10]. These cells have been assumed to share some close biological characteristics, such as self-renewal, multi-differentiation capacities, and surface epitopes, irrespective of the original source. Of these cells, BM-MSCs have received more attention in the field of regenerative medicine because of their specific advantages, such as low immunogenicity, rapid proliferation, and multi-lineage differentiation abilities [11]. Despite the extensive exploration and application of BM-MSCs due to its obvious merits serving as seed cells for tissue engineering or cell therapy, in consideration of the lineage “imprinting” effect [12, 13], it might be more suitable to adopt IVD-derived stem cells for IVD regenerative therapy. So it is necessary to identify new seed cell sources in IVD and make a comparison with the “classic” BM-MSCs concerning the biological characteristics.

Currently, several types of stem or progenitor cells have also been identified from different anatomical regions of IVDs. Risbud et al. [14] first identified a population of skeletal progenitor cells from human degenerate NP and suggested the progenitors might be used to treat disc

degenerated disease (DDD). In addition, Blanco et al. [15] also isolated a type of MSC-like stem cells from degenerate lumbar NP and demonstrated that these cells fulfilled the criteria for MSCs described by the ISCT with the exception of the ability to differentiate into adipocytes. Feng et al. [16] isolated a type of MSCs from the AF of human IVD, and these cells could differentiate into adipocytes, chondrocytes, osteoblasts, neurons, and endothelial cells. Additionally, we have also determined the presence of MSC-like cells with multi-lineage differentiation abilities in the CEP of degenerated human IVD (CESCs) and explored its preliminary biological characteristics [17, 18]. To localize the origin of stem cells in IVD, Helena B et al. investigated normal and degenerated discs from four species including human, and found that AF outer region located near ligament attachment and perichondrium region should be the potential stem cell niche in IVD [19]. Recent study, furthermore, confirmed the presence of local mesenchymal progenitor cells in human degenerated IVD [20]. In addition, AF and NP cells isolated from human degenerated IVD were further separated into single and clustered cells, and both cell populations contained a similar proportion of cells with stem cell or progenitor cell properties [21].

To date, no study has compared the biological characteristics of these stem cells (AFSCs, NPSCs, CESCs and BM-MSCs) from the same individual. Furthermore, the more adaptive application relative to its superior biological properties *in vitro* is also unknown. Therefore, in this study, we characterized the differences in the previously described stem cells regarding proliferative capacity, surface epitopes and multi-lineage differentiation abilities.

Furthermore, the potential NP tissue engineering application (composed with alginate) in vitro was examined in DNA content, sGAG excretion and histology. Through quantitative and qualitative comparisons, we expect to identify the variant biological characteristics and explore the most suitable application for regenerative medicine based on these properties. In addition, the elucidation of basic cell characteristics will lay a foundation for further investigations of the underlying IVD degeneration mechanism.

Materials and methods

Case selection

IVD tissues (AF, NP and CEP) and bone marrows were obtained from 11 donors who underwent spinal fusion surgery for DDD (Table 1). The age of the donors ranged from 41 to 57 years (average years: 47.0 ± 0.2), and the details are shown in Table 1. Informed consent and approval for sample collection were obtained from the Institutional Review Board and the donors prior to surgeries. All research protocols were conducted in compliance with the Helsinki Declaration. All the 11 cases received Transforaminal Lumbar Interbody Fusion (TLIF) procedures.

Histologic analysis

AF, NP and CEP were fixed in 10 % formalin at room temperature for 24 h, embedded in paraffin and sectioned to 5- μ m-thick sections. Different tissue slices were stained with H&E to indicate their histological features (Fig. 1).

Isolation and culture of human BM-MSCs

The isolation protocol of BM-MSCs was performed according to previously published papers [22, 23]. Bone

marrow was aspirated from the iliac crest of the donors and loaded into Percoll solution (1.073 g/ml, Sigma, USA) to obtain mononuclear cells (MNCs) by density gradient centrifugation at 900 g for 25 min. The obtained MNCs were rinsed twice with phosphate-buffered saline (PBS) and subsequently resuspended with Dulbecco's modified Eagle's medium/F12 (DMEM/F12, Hyclone, USA) supplemented with 10 % fetal calf serum (FCS, Hyclone, USA) and 100 U/ml penicillin–streptomycin (Hyclone, USA); the cells were ultimately seeded in a 25-cm² culture flask (Costar Corning, USA) at a density of 1×10^6 cells/cm². After 72 h in 5 % CO₂ at 37 °C, the non-adherent cells were removed by refreshing the medium, and the remaining cells were continuously cultured with medium that was changed every 3 days. When 90 % confluence was attained, the cells were passaged.

Acquisition and culture of AF-derived cells, NP-derived cells and CEP-derived cells

The IVD samples (which contained AF, NP and CEP) were separated by an experienced surgeon; the AF, NP and CEP tissues were then accurately acquired using an anatomy microscope (4 \times magnification). The tissues were dissected into fragments less than 1 mm³ and subsequently digested with 0.2 % type II collagenase (Sigma, USA) at 37 °C for 6 h. These cells (AF, NP and CEP cells) were obtained by filtering with a 200-well filter and then seeded in a 25-cm² culture flask with the previously described medium.

Agarose culture

To obtain cell clusters, an agarose suspension culture system was used in this study as previously described [18, 24]. The culture dishes (60 mm in diameter) were first coated with 1 % low-melting point agarose, which contained equal volumes of DMEM/F12 and 2 % low-melting point agarose; the superfluous agarose was removed. For

Table 1 Characteristic details of the patients enrolled in this study

Case No.	Age (years)	Gender	Symptoms	Diagnosis	Disc level	Pfirrmann grading
Case 1	49	M	BP	Lumbar discogenic pain	L4/5	IV
Case 2	44	F	BP–RP	Spondylolisthesis	L5/S1	III
Case 3	57	M	BP–RP	Lumbar disc herniation	L5/S1	III
Case 4	46	F	BP–RP	Lumbar disc herniation	L4/5	III
Case 5	49	M	BP–RP	Lumbar disc herniation	L5/S1	III
Case 6	41	M	BP	Spondylolisthesis	L5/S1	IV
Case 7	42	F	BP	Spondylolisthesis	L4/5	IV
Case 8	46	F	BP	Lumbar discogenic pain	L4/5	III
Case 9	45	M	BP–RP	Lumbar disc herniation	L4/5	IV
Case 10	47	M	BP–RP	Lumbar disc herniation	L5/S1	III
Case 11	52	F	BP–RP	Spondylolisthesis	L5/S1	IV

BP back pain, RP radicular pain

preparation, approximately 1×10^5 different types of passage 2 cells were suspended with 1.5 ml of 20 % FCS DMEM/F12. Then, a 1.5 ml mixture of 0.75 ml DMEM/F12 and 0.75 ml of 2 % low-melting point agarose was added to the cell solution. The final mixture was inoculated in the coated dishes and incubated in 5 % CO₂ at 37 °C. The culture media were refreshed twice per week. The cell clones formed after approximately 6 weeks and were transferred to a 25-cm² culture flask for subculturing. Usually 1×10^3 to 1×10^4 stem cells could be isolated, respectively, from the corresponding IVD samples of one patient.

To fulfill the large amounts of cells needed for each part of the experiment, each kind of stem cells derived from 3 donors were pooled for measurement of cell proliferation capacities and determination of the cell surface antigen profile, stem cells from 5 donors were mixed for comparison of differentiation capacities, and stem cells from 3 donors were pooled for construction of stem cell-alginate bead composition.

Determination of the cell surface antigen profile

To analyze the surface immunophenotype, the passage 2 cells were examined by flow cytometry. Briefly, the cells were washed with PBS twice and incubated for 20 min in the dark at room temperature with fluorescein isothiocyanate (FITC)-, peridinin chlorophyll protein (PerCP)-, and allophycocyanin (APC)-coupled monoclonal antibodies, including: CD19-APC, CD34-FITC, CD45-FITC, CD73-FITC, CD90-FITC, CD105-FITC, and HLA-DR-PerCP. All antibodies were purchased from eBioscience (Santa Cruz Biotechnology, USA). The cells were washed with PBS twice again, resuspended in 200 µl PBS, and then passed through a Flow Cytometer. The antigen phenotype was analyzed using FlowJo software (FlowJo, USA). Mouse isotype antibodies served as controls. Triplicate cells were analyzed for each antigen phenotype.

Morphological characteristics and measurement of cell proliferation capacity

The morphological characteristics of the different cell types and corresponding passages were identified and photographed using a phase contrast microscope (Olympus, Japan).

The proliferation capacities were measured by counting the cell numbers. P2 cells were seeded in a 6-cm-diameter dish (8000 cells/cm²) and cultured for 1, 3, 5, 7, 9, 11, and 13 days; the cell number was then calculated. Three replicate wells were set for each measurement, and the mean value was used to evaluate their proliferation capacities.

Osteogenic differentiation

The cells (80 % confluent) were seeded on 24-well culture plates and incubated for 24 h; the normal culture media were then replaced with osteogenic induction media (Osteogenesis Differentiation Kit, GIBCO, USA). The induction process lasted for 21 days and the media were changed every 3 days. The control cells were maintained in DME/F12 with 10 % FCS. Finally, the induction media were removed, and the cells were rinsed with PBS, followed by fixation with a 4 % paraformaldehyde–glutaraldehyde solution at room temperature for 1 h for alizarin red staining.

Chondrogenic differentiation

A pellet culture was employed for chondrogenic induction as previously described [25]. The cells (3×10^6 per cell type) were centrifuged at 500 g for 10 min in a 15-ml polypropylene tube to form a pellet. Without being disturbed, the cell pellets were incubated for 24 h with normal medium; the normal medium was subsequently replaced by chondrogenic induction medium (Chondrogenic Differentiation Kit, GIBCO, USA). Thereafter, the induction medium was refreshed every 3 days. Blank controls were cultured with DMEM/F12 with 10 % FCS. On day 14, the cell aggregates were weighed to determine the wet weights and fixed in 4 % paraformaldehyde–glutaraldehyde solution for 15 min at room temperature; the cells were then dehydrated in serial ethanol solutions and embedded in paraffin blocks. The paraffin sections (5 µm thick) were stained with alcian blue dye for histological analysis.

Adipogenic differentiation

The cells were seeded in 24-well culture plates and incubated for 24 h; the normal medium was subsequently replaced by adipogenic induction medium (Adipogenic Differentiation Kit, GIBCO, USA). The negative controls were maintained in normal medium. On day 21, the cells layers were fixed with 4 % paraformaldehyde–glutaraldehyde solution for 15 min at room temperature and stained with oil red O for an additional 15 min to confirm the newly formed lipid droplets. After thoroughly removing the redundant dye with water, the droplets were observed and photographed using microscopic inspection (Leica, Germany).

Semi-quantitative assay of alkaline phosphatase (ALP) activity

To evaluate the ALP activity, a modified procedure was used as previously described [26]. After 21 days of

induction in a 96-well plate (1×10^4 cells seeded per cell type), the osteo-induced cells were carefully washed with PBS, incubated in a mixed solution, which contained 1.0 mM $MgCl_2$, 6.7 mM p-nitrophenyl phosphate (pNPP) and 25 mM ethanolamine for 30 min, and then terminated by a 100 μ l NaOH solution (0.1 mM). Finally, these plates were tested for the optical density (OD) values at 405 nm using a spectrophotometer. The quantitative ALP activity was determined by the OD intensity. Three replicate wells were set for each cell type, and the mean OD value was used to evaluate the ALP activity.

Semi-quantitative assay of mineral deposits

This protocol was performed according to a previous paper [18]. Cells (1×10^5 cell per cell type) were seeded in each well of a 12-well plate and then induced in an osteogenic medium for 21 days. After induction, the cells were carefully washed with PBS twice and fixed in ethanol (70 %, w/w) for 40 min at room temperature. The cells then were stained with alizarin red staining for 15 min and then washed with distilled water three times. Finally, they were incubated with 600 μ l cetylpyridinium chloride solution (10 %, w/w) at room temperature for 15 min; the OD value at 562 nm was subsequently measured using a spectrophotometer. Three replicate wells were set for each cell type, and the mean OD value was used to evaluate the mineral deposits.

Semi-quantitative assay of alcian blue intensity

All procedures were performed as previously described [27]. After induction for 14 days, the chondro-induced cell pellets (3×10^6 cell initially seeded per cell type) were washed twice with PBS, fixed with 10 % neutral buffered formalin, including 1 % cetylpyridinium chloride (CPC), for 15 min, and then washed with PBS again; they were then stained with 1 % alcian blue 8GS, which was dissolved in 0.1 M HCl, for 1 h. To quantify the alcian blue intensity, these cultures were rinsed with 50 mM Tris–HCl and incubated with a 300 μ l solution, which contained 4 M Guanidine–HCl, 50 mM Tris–HCl and 0.1 % Chaps, for 2 h at room temperature. The OD value of the extracted dye was tested at 595 nm using a spectrophotometer. Three replicate pellets were set for each cell type, and the mean OD value was used to evaluate the alcian blue intensity.

Semi-quantitative assay of adipogenic capacity

The adipogenic capacity was quantitatively measured according to a previously described protocol [18, 28]. This protocol was based on the lipid-rich vacuoles with oil red O staining, and the OD value was positively correlated with

the staining intensity. After adipo-induction for 21 days in 96-well plates, the cells (1×10^4 cell per cell type) were cleaned, fixed, and dyed with oil red O and then lysed on a shaking table at 30 reverse/min for 30 min. The OD value of dye extracts were tested at 490 nm using a spectrophotometer. Three replicate wells were set for each cell type, and the mean OD value was used to evaluate the adipogenic capacity.

Real-time quantitative reverse transcriptase polymerase chain reaction (qPCR) assay

To compare the osteogenic-, chondrogenic-, and adipogenic-specific gene expression levels of different cell types, quantitative PCR was performed after the cells had been induced as previously described. Briefly, the total RNA was extracted using an RNase kit (Qiagen GmbH, Germany) according to the manufacturer's instructions. RNA was measured to determine the 260/280 nm absorbance ratio (>1.8) using a spectrophotometer and treated with RNase-free DNase prior to reverse transcription into cDNA. Reverse transcription was performed using the High-Capacity cDNA Reverse Transcription Kit (Applied Biosystems, Foster City, CA). Housekeeping β -actin was utilized to normalize the reactions.

The primers were designed using Primer Express software (PE Applied Biosystems) and are listed in Table 2. The reverse transcriptase polymerase chain reaction (RT-

Table 2 Primer sequences in the qPCR analysis

Gene name	Primer sequence
<i>β-actin</i>	5'-GTGGGGCGCCCCAGGCACCA-3' (forward) 5'-CTTCCCTAATGTCACGCACGATTTTC-3' (reverse)
<i>Sox-9</i>	5'-TGGCCGAGATG ATCTAAAAATAA-3' (forward) 5'-GCGCTTGATAGGTCATGTTTGT-3' (reverse)
<i>Aggrecan</i>	5'-TGGAGGTGGTGGTAAAGGTGT-3' (forward) 5'-GGCGTCGCACTGGTGGAA-3' (reverse)
<i>Collagen II</i>	5'-CCTTCCTGCGCCTGCTGTC-3' (forward) 5'-GGCCCGGATCTCCACGTC-3' (reverse)
<i>OC</i>	5'-ATGAGAGCCCTCACACTCCTC-3' (forward) 5'-GCCGTAGAAGCGCCGATAGGC-3' (reverse)
<i>Runx-2</i>	5'-ACGACAACCGCACCATGGT-3' (forward) 5'-CTGTAATCTGACTCTGTCT-3' (reverse)
<i>ALP</i>	5'-TGGAGCTCAGAAGCTCAACACCA-3' (forward) 5'-ATCTCGTTG TCTGAGTACCAGTCC-3' (reverse)
<i>LPL</i>	5'-TCCGCGTGATTGCAGAG AGAG-3' (forward) 5'-TGCTGCTTCTTTGGCTCTGACT-3' (reverse)
<i>PPAR-2</i>	5'-CGAGGGCGATCTTGACAGGAA -3' (forward) 5'-CAGGGGGGTGATGTGTTTGAAC- 3' (reverse)
<i>APP</i>	5'-CTGTCCAAGTCCAACAGCAA-3' (forward) 5'-ACGTTGGCAGCTTTACGTCT-3' (reverse)

PCR) products were resolved for 1 % agarose gel electrophoresis and visualized using a gel imaging system (BioRad, America). To calculate the relative expression of each target gene, the $2^{-\Delta C_t}$ method was used as described in previous papers [29–31]. Each sample was tested three times per gene.

Construction of stem cell–alginate bead composition

The stem cells were trypsinized, centrifuged at 1000 rpm/min for 5 min and rinsed twice with PBS. After the supernatant was carefully aspirated away, an appropriate volume of alginate (1.2 % w/v) was added and blended to obtain a mixture at a cell density of 3×10^6 /ml. The mixture was sucked into a 5-ml syringe and dropped through the syringe pinhole into a 6-well culture plate, which contained a calcium chloride solution at a concentration of 35 g/L in advance. After cross-linking with calcium chloride for 20 min, the cell/alginate composition changed into spherical beads and floated in the calcium chloride solution. The beads were subsequently washed twice with PBS and cultured with fresh normal culture media. During culturing, the medium was refreshed twice in 1 week.

DNA content and proteoglycan measurement

The DNA content was tested as previously described [32]. On days 1, 7, 14 and 28 after construction, the beads were incubated in a papain buffer solution (Sigma, America) (200 μ l per bead) at 60 °C for 24 h. After incubation, 100 μ l of the digested solution was mixed with 1 ml Hoechst 33,258 dye (Sigma, America); then, 200 μ l of mixture was sucked into the well of a 96-well plate and tested with excitation at 365 nm and emission at 458 nm using a microplate absorbance reader (BioRad, America). A standard curve was also elaborated from known concentrations of calf thymus DNA (Sigma, America) to quantify the DNA content. Three replicate beads were set for each measurement, and the mean value was used to evaluate the DNA content at each time point.

The sulfated glycosaminoglycan (sGAG) content was detected according to the prescribed protocol [33]. 40 μ l of papain digestive juice of the digestive bead was sucked into the 96-well plate, which included 1,9-dimethylmethylene blue dye (DMMB) at pH 3. After mixing, the OD value at 595 nm was measured using the microplate absorbance reader. The final sGAG content was determined through comparison with the linear standard curve, which was elaborated from the known concentrations of chondroitin-6-sulfate (6-CS). Three replicate beads were set for each measurement.

Histomorphology and scanning electron microscope (SEM) observations

On day 28, the beads were fixed with 10 % neutral buffered formaldehyde solution for 48 h, dehydrated by a graded ethanol series, embedded in paraffin and sectioned at 5 μ m thickness using a microtome. These slices were subsequently stained with toluidine blue for observation. Beads without cells were used as a control.

In addition, beads cultured for 28 days were first fixed with a 4 % paraformaldehyde and glutaraldehyde solution, which contained 0.1 M cacodylate buffer, for 8 h at room temperature and rinsed twice with a 50 mM CaCl_2 buffer solution. The beads were subsequently dehydrated by a graded ethanol series, sputtered with gold followed by critical-point drying, and finally observed using SEM (HITACHI, Japan).

Statistical analysis

The data are presented as the mean \pm SD. One-way analysis of variance (ANOVA) was conducted to analyze the differences among different cell types. $p < 0.05$ was considered statistically significant.

Results

Morphological observation and cell proliferation capacity

At passages 1 and 2, the CEP-derived cells exhibited a relatively round shape. The AF-derived cells and BM-MSCs shared a similar configuration to the long, spindle-shaped fibroblasts, whereas the NP-derived cells exhibited a polygonal morphology. For the stem cells, they all shared a similar shape. However, compared with the NPSCs and CESC, the BM-MSCs and AFSCs exhibited a relatively long and slender figure (Fig. 2a).

Regarding the proliferation capacity, all cell types exhibited similar growth tendencies. The stem cell number increased from day 1 to 13 and entered a slow growth period from day 11. Although the BM-MSCs exhibited a relatively stronger proliferation potential and the AF-derived cells were the weakest in comparison at each time point, there were always no significant differences among them ($p > 0.05$) (Fig. 2b).

Immunophenotypic characterization

All stem cells shared a similar surface immunophenotypic profile. They were negative for CD19, CD34, CD45 and HLA-DR (<2.0 %), and no significant differences were

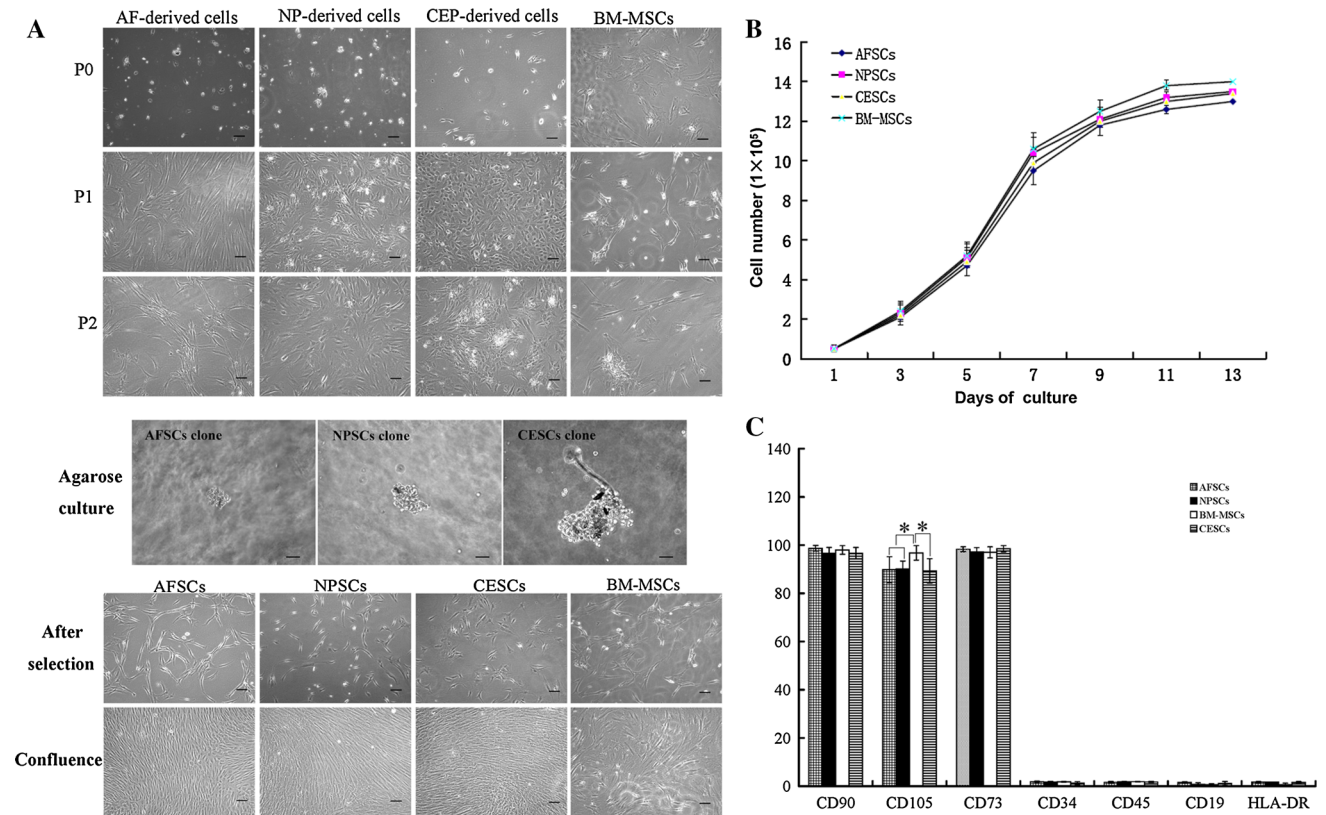


Fig. 2 Biological characteristics of the four cell types. **a** Microscopic features of the cells derived from different anatomical regions, stem cell clones and expanded stem cells. **b** Proliferation capacities.

c Immunophenotypic profiles. Data are presented as the mean ± SD. **p* < 0.05 (Bar 100 μm)

identified for CD19 (*p* > 0.05), CD34 or CD45 (*p* > 0.01); however, the BM-MSCs expressed significantly lower HLA-DR than the AFSCs, NPSCs and CESC (*p* < 0.05). CD90 and CD73 were highly expressed in all types of stem cells (>95 %), and no significant differences were identified among the four types cells (*p* > 0.05). As for CD105 expressed in the AFSCs, NPSCs, CESC and BM-MSCs, it was 89.80 ± 3.08, 94.20 ± 2.40, 89.30 ± 2.20 and 96.80 ± 1.41, respectively. Statistically significant differences were identified between BM-MSCs and NPSCs, and between NPSCs and AFSCs or CESC (*p* < 0.05) (Fig. 2c).

Osteogenic differentiation

Osteogenic differentiation was demonstrated by the mineralization of the extracellular matrix stained with Alizarin Red and the calcium deposition in the different stem cells after 3 weeks of induction. By rough observation, the CESC appeared to form more intensely stained mineralized nodules (Fig. 3a).

The quantitative assay for ALP activity demonstrated that the OD value of the CESC group was the highest (3.77 ± 0.31) followed sequentially by the AFSCs

(3.13 ± 0.32), BM-MSCs (3.12 ± 0.28) and NPSCs (2.70 ± 0.37). The results indicated that there were significant differences between the CESC and any two groups (*p* < 0.05) (Fig. 3b).

The dye absorption (562 nm) indicated that the alizarin red-positive mineralized matrices of the CESC was the most (1.76 ± 0.27), and the AFSCs were slightly more than the BM-MSCs (1.45 ± 0.20 vs. 1.43 ± 0.18); the NPSCs were the least (1.12 ± 0.22). A significant difference was identified between the CESC and any other type of stem cells (*p* < 0.05). However, among the other three types of stem cells, a significant difference existed between any two groups (*p* < 0.05), with the exception of the AFSCs vs. BM-MSCs (*p* > 0.05) (Fig. 3c).

According to the results of the qPCR assay, significant differences were identified between any two types of stem cells (*p* < 0.001) for the ALP expression level. The CESC was the highest (1.76 ± 0.18-fold), followed by the AFSCs (1.00 ± 0.18), BM-MSCs (0.27 ± 0.081) and NPSCs (0.07 ± 0.024). The same trends were also identified for OC and Runx-2 despite the lack of a significant difference when the BM-MSCs (0.27 ± 0.08) and NPSCs were compared (*p* > 0.05) (Fig. 3 d, e).

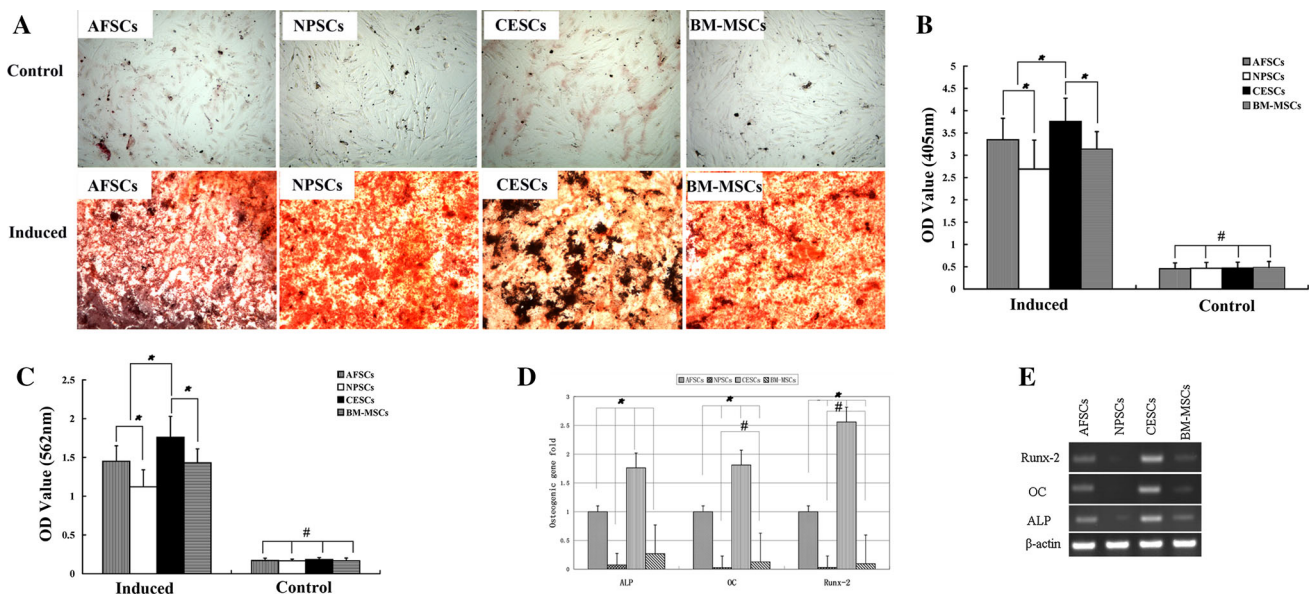


Fig. 3 Osteogenic potentials of AFSCs, NPSCs, CESC and BM-MSCs. **a** Histological appearances with alizarin red staining. **b** Quantitative assay of ALP activity. **c** Quantitative assay of mineral deposits. **d** Quantitative expression analysis of osteogenic-specific

genes by qPCR. **e** RT-PCR of osteogenic specific genes. AFSCs annulus fibrosus-derived stem cells, NPSCs nucleus pulposus-derived stem cells, CESC cartilage endplate-derived stem cells. Data are presented as the mean \pm SD. * $p < 0.05$; # $p > 0.05$ (Bar 100 μ m)

Chondrogenic differentiation

After chondrogenic differentiation in the pellet culture system, the histological observation demonstrated that all stem cells exhibited intense staining of sulfated proteoglycan (Fig. 4a, b). After an induction of 14 days, the wet weight of the CESC pellets (4.22 ± 0.18 mg) was the heaviest, followed by the AFSCs (3.42 ± 0.22 mg), BM-MSCs (3.32 ± 0.21 mg) and NPSCs (2.97 ± 0.20 mg). Significant differences were identified between any two groups ($p < 0.05$) (Fig. 4c). The quantitative assay for sulfated proteoglycan indicated that the OD value of the CESC group was the highest (0.33 ± 0.08), followed by the AFSCs (0.26 ± 0.05), BM-MSCs (0.21 ± 0.05), and NPSCs (0.21 ± 0.04). There were significant differences between any two groups ($p < 0.05$), with the exception of the BM-MSCs vs. NPSCs ($p > 0.05$) (Fig. 4d).

The results of the qPCR assay indicated that chondrogenic-specific genes (SOX-9, Aggrecan and Collagen II) were expressed in all groups. Regarding the expression of SOX-9, the CESC had the highest expression (1.22 ± 0.12 -fold), followed by the AFSCs (1.00-fold) and BM-MSCs (0.98 ± 0.14 -fold); the NPSCs had the lowest expression (0.76 ± 0.14 -fold). Significant differences were identified when the CESC or NPSCs were compared with any other group ($p < 0.05$); however, no significant difference was identified between the AFSCs and BM-MSCs ($p > 0.05$). For aggrecan expression, the CESC also had the highest expression (1.41 ± 0.12 -fold), and significant differences were

identified between any other group ($p < 0.05$), with the exception of the AFSCs vs. BM-MSCs ($p > 0.05$). The CESC had the highest collagen expression (1.48 ± 0.09 -fold), which was followed by the BM-MSCs (1.25 ± 0.07), AFSCs (1.00) and NPSCs (0.79 ± 0.11). Significant differences were identified between any two groups ($p < 0.001$) (Fig. 4e, f).

Adipogenic differentiation

All stem cells exhibited intracellular lipid vacuoles with red O staining after 21 days of adipogenic induction (Fig. 5a). The quantitative assay indicated that the OD value of the BM-MSC group was the highest (0.12 ± 0.05), followed by the NPSCs (0.11 ± 0.05), CESC (0.10 ± 0.04), and AFSCs (0.10 ± 0.07). There were significant differences between the BM-MSCs and any other stem cell type ($p < 0.001$); furthermore, a significant difference was also identified between the AFSCs and NPSCs ($p < 0.01$). When the CESC were compared with the NPSCs or AFSCs, no significant difference was identified ($p > 0.05$) (Fig. 5b).

According to the qPCR results, the gene expression levels for adipogenic-specific genes (APP, LPL and PPAR-2) had the same trend among all stem cell types. All genes were expressed at the highest levels in the BM-MSCs with significant differences compared with any other group ($p < 0.001$). The three gene expression levels were the lowest in both the AFSCs and CESC with no significant difference between them ($p > 0.05$). (Fig. 5c, d).

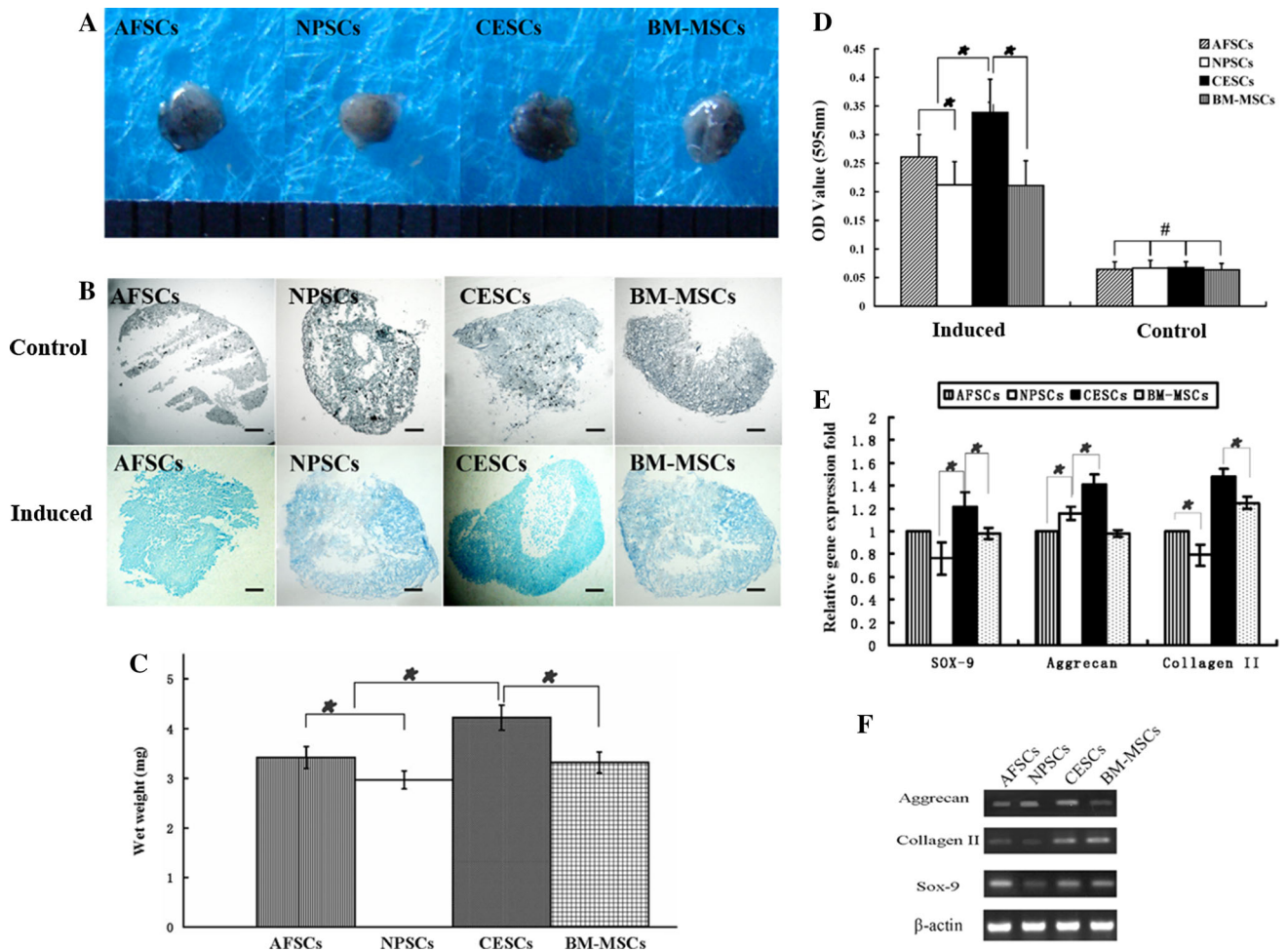


Fig. 4 Chondrogenic potentials of AFSCs, NPSCs, CESC and BM-MSCs. **a** Representative gross appearances of cell pellets after induction. **b** Histological appearances stained by alcian blue staining. **c** Wet weights of the pellets from different types of stem cells.

d Quantitative assay of alcian blue intensity. **e** Quantitative expression analysis of chondrogenic-specific genes by qPCR. **f** RT-PCR of osteogenic-specific genes. Data are presented as the mean ± SD. * $p < 0.05$; # $p > 0.05$ (Bar 100 μm)

Biochemical characteristics of stem cells/alginate compounds

Over time, the DNA contents of all cell types presented a consistent, increasing tendency. At the 7-day time point, the amounts of DNA in the CESC group was the highest (51.46 ± 2.65 ng/mg), followed by the BM-MSC group (51.28 ± 2.38 ng/mg); both the AFSCs–alginate and NPSCs–alginate compounds were the lowest (48.21 ± 2.85 and 50.09 ± 2.46 ng/mg, respectively). On day 14, the DNA content increased from the 7-day time point to 70.05 ± 2.29 ng/mg (BM-MSC group), 68.57 ± 2.62 ng/mg (CESC group), 67.33 ± 2.40 ng/mg (NPSC group) and 65.81 ± 3.05 ng/mg (AFSC group), respectively. At the 28-day time point, the DNA content in all groups had continued to increase to 76.27 ± 2.20 ng/mg (BM-MSC group), 74.58 ± 2.51 ng/mg (CESC group), 74.14 ± 2.20 ng/mg (NPSC group) and 72.36 ± 2.75 ng/mg

(AFSC group), respectively. However, at all four time points, no significant group differences were identified from start to finish ($p > 0.05$) (Fig. 6a).

Regarding the sGAG that accumulated on the scaffold, a similar trend was identified compared with the DNA content. At the day 1 time point, all cells exhibited close amounts (AFSCs, 2.31 ± 0.45 ng/mg; NPSCs, 2.38 ± 0.42 ng/mg; CESC, 2.45 ± 0.40 ng/mg and BM-MSCs, 2.4 ± 0.41 ng/mg). At the 7 day time point, the amount of sGAG in the CESC group was the highest (5.31 ± 0.60 ng/mg), followed by the BM-MSC group (5.1 ± 0.35 ng/mg); both the AFSC and NPSSC groups were the lowest (4.56 ± 0.27 ng/mg and 4.82 ± 0.28 ng/mg, respectively). At the two time points, no significant differences were identified between any groups ($p > 0.05$). At 14-day time point, the sGAG of the CESC group increased to 9.88 ± 0.65 ng/mg and was significantly higher than the other groups (AFSCs, 8.14 ± 0.35 ng/mg;

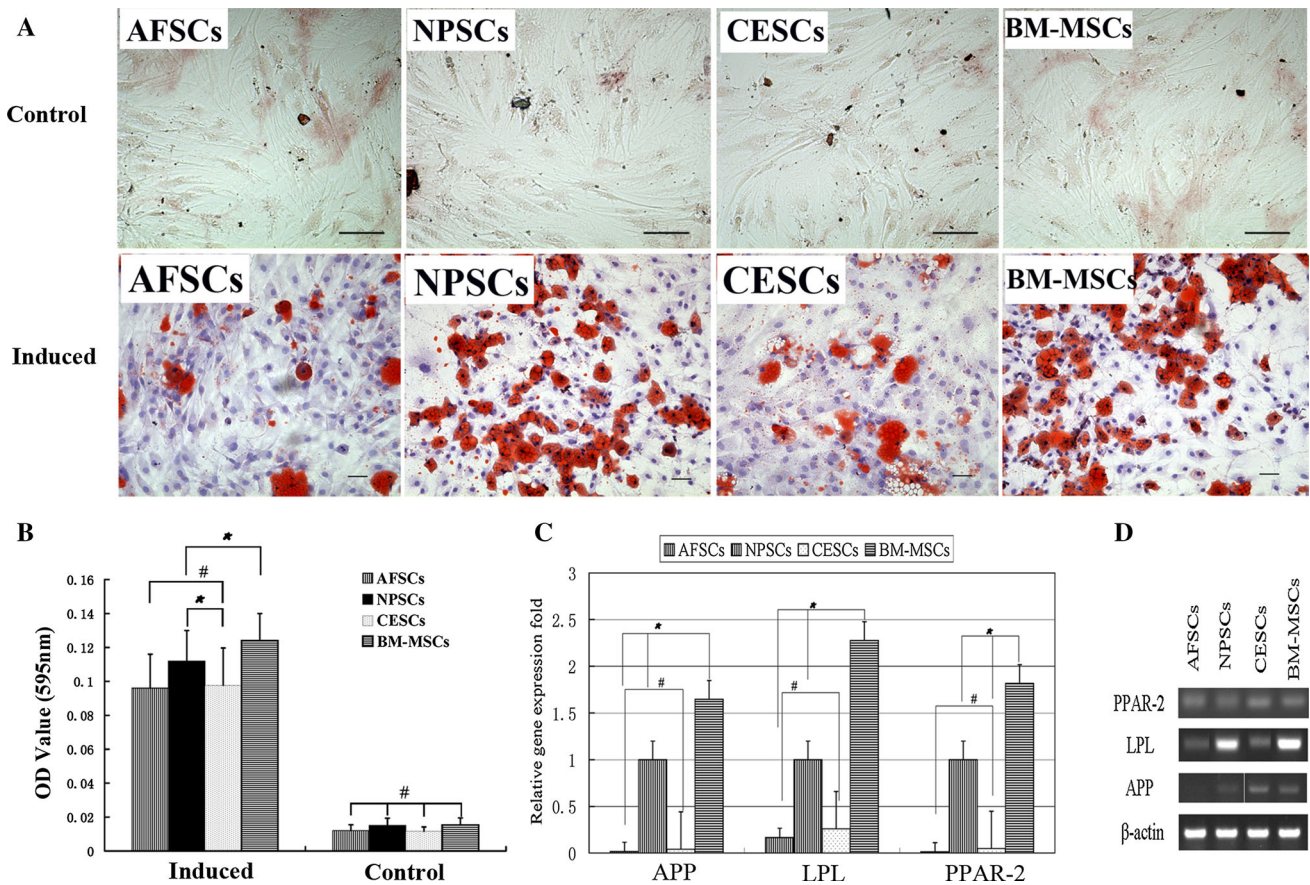


Fig. 5 Adipogenic potentials of AFSCs, NPSCs, CESC and BM-MSCs. **a** Histological appearances with oil red O staining. **b** Quantitative assay of adipogenic capacity. **c** Quantitative expression

analysis of adipogenic-specific genes by qPCR. **d** RT-PCR of adipogenic-specific genes. Data are presented as the mean \pm SD. * $p < 0.05$; # $p > 0.05$ (Bar 100 μ m)

NPSCs, 8.56 ± 0.32 ng/mg; and BM-MSCs, 9.24 ± 0.28 ng/mg ($p < 0.05$). Until 28 days, the sGAG of the CESC group increased to 11.42 ± 0.45 ng/mg and remained significantly higher than any other group (AFSCs, 10.10 ± 0.25 ng/mg; NPSCs, 10.35 ± 0.36 ng/mg; and BM-MSCs, 10.76 ± 0.38 ng/mg) ($p < 0.05$) (Fig. 6b).

Morphological observation for stem cell/alginate bead

After 28 days of culture, toluidine blue staining revealed that the cell/alginate beads had an inner poly porous structure, which was dyed brown, and the dimensions of the pores were inhomogeneous. Through the transverse section under $100\times$ magnification, several blue-dyed cell clusters adhered to the scaffold were identified and wrapped by secreted ECM (Fig. 6c).

In the SEM observation, the beads exhibited an oval gross appearance. One day after construction, the cells had adhered to the alginate scaffold, but no obvious ECM was

secreted (Fig. 6d). At the 28-day time point for all cell types, large amounts of latex-like ECM had accumulated around the cells, and the cell outline was hardly recognized (Fig. 6e).

Discussion

In this study, for the first time, we performed a side by side comparison of MSCs (AFSCs, NPSCs, CESC and BM-MSCs) derived from different anatomical regions of degenerated intervertebral discs and bone marrow from the same donors regarding general biological characteristics and the potential application for tissue engineering. Our results demonstrated that the four types of stem cells shared similar morphologies, proliferation abilities, and surface immunophenotypes. The osteogenic and chondrogenic differentiation capacities were as follows: CESC $>$ AFSCs $>$ BM-MSCs $>$ NPSCs; however, for the adipogenic differentiation potential, the BM-MSCs differentiated most readily into adipocytes, followed by the

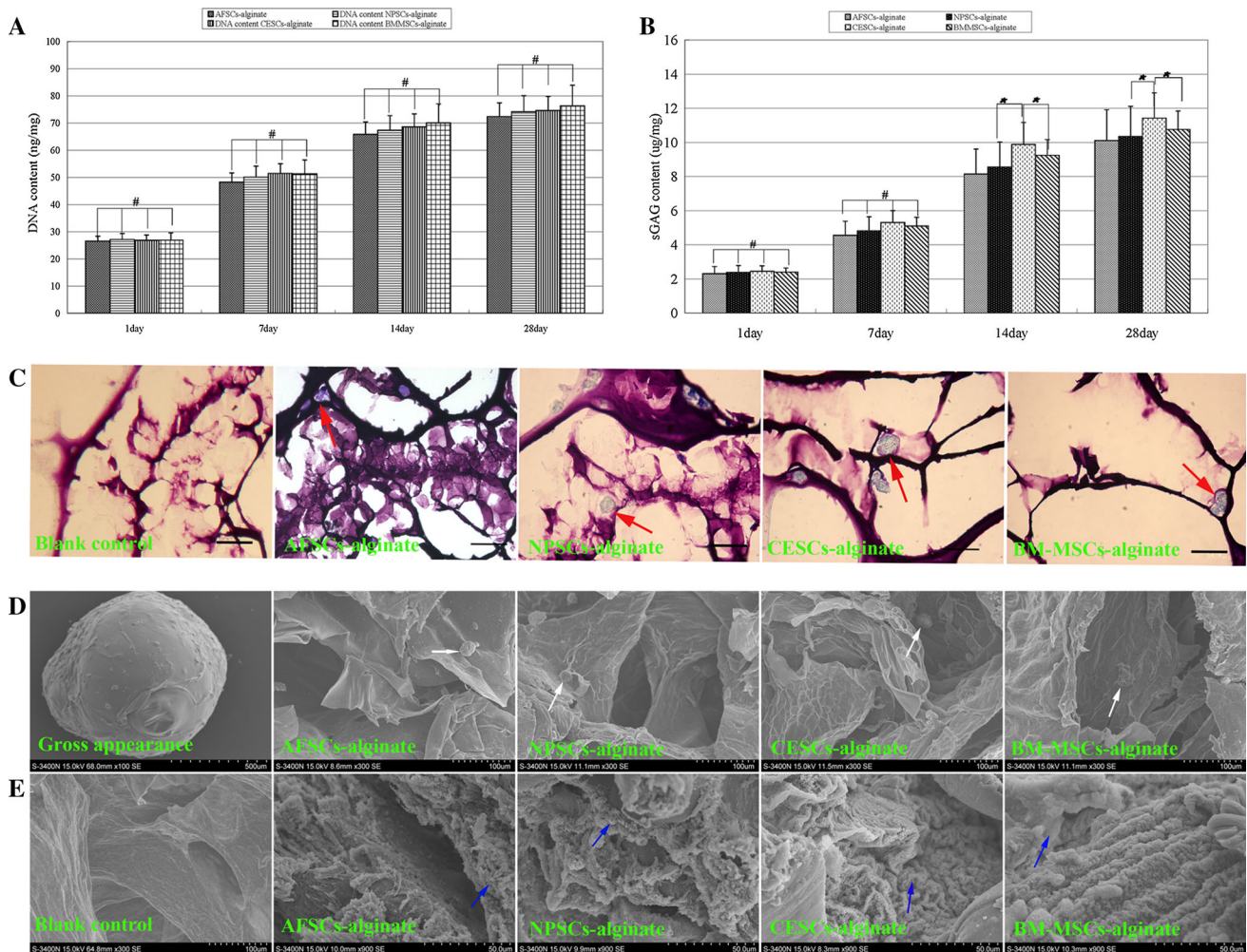


Fig. 6 Biochemical characteristics of stem cells/alginate compounds. **a** DNA contents at different time points. **b** sGAG contents at different time points. **c** Histological appearances with toluidine blue staining. **d** SEM observation on day 1 after construction. **e** SEM observation on

day 28. *Red arrow* indicates the cell clusters wrapped by secreted ECM; *White arrow* indicates the seeded cells adhered to the scaffold; *Blue arrow* indicates the accumulated ECM. Data are presented as the mean ± SD. **p* < 0.05; #*p* > 0.05 (Bar 100 µm)

NPSCs, CESC and AFSCs with an inferior capacity. In addition, when serving as seed cells, all stem cells demonstrated the basic biological properties in alginate scaffold, especially the CESC, which exhibited the most robust sGAG secretion ability.

In theory, large amounts of IVD tissues could be obtained by anterior lumbar interbody fusion (ALIF) procedure, and each anatomical part of resected IVD was easy to be identified and separated. However, ALIF is not the routine procedure for DDD. When comparing with ALIF, most spine surgeons are more familiar with posterior lumbar interbody fusion (PLIF) and TLIF. For PLIF, the facet joint is reserved, and the more medial approach makes it hard to avoid the posterior longitude ligament (PLL), which mixes PLL tissue into the harvested AF sample. In TLIF procedures, after resecting the facet joint, the posterolateral surface of AF could be directly observed and approached in the

region of intervertebral foramina, and the PLL could be avoided due to the relatively lateral approach. Only the top layers of AF in this region were obtained as samples to ensure unique AF tissue. For NP samples, only loose tissues were harvested from the “core” of disc space to prevent the adjacent AF tissues encroached. CEP tissues were easy to be identified with specific morphological structures. To ensure the unique tissue samples, any indefinite tissues which were hard to be distinguished macroscopically or microscopically had been discarded.

The agarose suspension culture is a mature and reliable protocol in which only tumor, transformed, or stem cells can survive and proliferate in the clone shape [24, 34]. Using this method, all three kinds of IVD stem cells could form cell clones in the agarose after approximately 6 weeks. The selected cells were confirmed by the surface immunophenotype analysis and multi-lineage induction

abilities. After selection, all stem cells tended to be homogeneous, and no significant differences were identified between groups regarding the proliferative potential, adhesive or tridimensional culture when mixed with alginate. For the colony formation efficiency, in our previous experience, cell clones were easy to form and showed strong proliferative ability in younger patients, but in older cases, especially around 70 years or older, cell clones seldom formed, and isolated cell clones proliferated slowly after transferred to a the culture flask for subculturing. So in this study, relatively young patients with age range from 41 to 57 years (average years: 47.0 ± 0.2) were enrolled, and for all the 11 cases, cell clones derived from different cell types were obtained. We did not focus on the specific colony formation efficiency in this study, but around 5–10 % colony formation efficiency could be achieved. In our next study, a study will be set up about the relationship between colony formation efficiency and age or the degree of disc degeneration.

We demonstrated that the stem cells closely expressed the MSC surface markers stated by the International Society for Cellular Therapy (ISCT) [35], in which the surface markers are positive for CD73, CD105, and CD90 and negative for CD34, CD45, CD19 and HLA-DR. CD105, a receptor for transforming growth factor- β (TGF- β), is primarily engaged in cell adhesion, spreading and migration; it is often moderately expressed in chondrocytes and highly expressed in cells with high migration abilities. The increased expression of CD105 may signify more prosperous capacities of homing and migration [15, 16, 36]. In this study, BM-MSCs expressed highest level of CD105 among the four kinds of stem cells, the differential expression of CD105 might be related to the following factors. Firstly, the isolation, passaging, and culture conditions may impact CD105 expression [37]. Secondly, the discrepancy in the epitope profile was correlated with the histological origin, in which cells are affected by the surrounding environment [15]. Thirdly, BM-MSCs might actually have stronger migration and homing abilities compared with IVD-derived stem cells, which clearly must be further explored.

Based on the results of the qPCR and semi-quantitative assays of ALP activity, both indexes consistently demonstrated that CESC had a superior in vitro osteogenesis capacity compared with the other groups. A pellet culture protocol is often employed to evaluate chondrogenic differentiation capacity. The wet weight of the pellet increases as the ECM accumulate; thus, the chondrogenic capacity is reflected by the pellet weight or the OD value of the dye absorbed in the pellet tissue section [18, 25, 38, 39]. In this study, according to the semi-quantitative assay of alcian blue intensity and the wet weight data, the CESC exhibited the most powerful ECM excretion capacity. For qPCR, the CESC always expressed the strongest level of

chondrogenic genes (Sox-9, Collagen II and Aggrecan). Sox-9 plays a more important role in chondrogenesis and promotes the latter two genes' expression and function in ECM production [40–42]. In the stem cell/alginate composition, the CESC consistently showed the superior chondrogenic potential, which is consistent with our previous in vivo study [43]. This finding is perhaps attributed to the lineage “imprinting” phenomenon [12, 13], in which stem cells derived from the cartilage might be more inclined to differentiate to chondrocytes.

We also demonstrated that all four types of stem cells were capable of differentiating into adipocytes; the BM-MSCs had an increased adipogenic ability compared with the IVD-derived stem cells. The reason might be as follows: human adult bone marrow contains an abundance of fat tissue, and the local fat tissue microenvironment directs the “fate” of the MSCs; thus, the BM-MSCs could have been preconditioned via the microenvironment and thus more predisposed toward an adipocyte lineage [25]. In addition, our results were incompletely consistent with the previous study, which indicated that the nucleus pulposus derived stem cells had no adipogenic potential [15].

One of the most important considerations in tissue engineering is to harvest the greatest amount of seed cells with the highest desired potential. In our daily clinical work, we could obtain abundant IVD samples, which were typically discarded as clinical waste tissues in routine spinal fusion surgeries [44]. Thus, CESC have a significant advantage in tissue engineering application because of their easy source availability, as well as their high chondrogenic and osteogenic potentials. Although the surgery modality may continuously provide an adequate seed cell source, numerous obstacles still exist that must be managed; for example, how to prevent the attenuation of the proliferation and lineage induction abilities caused by serial passage, whether to avoid allograft rejection in the future potential clinical use, and how to store and transport the cells. In a future study, we would like to immortalize CESC and further investigate their potential applications in regeneration medicine [45].

Acknowledgments This work was supported by the National Natural Science Foundation of China (NSFC) (No. 81101364 and No. 81572186).

Compliance with ethical standards

Conflict of interest None.

References

1. Humzah MD, Soames RW (1988) Human intervertebral disc: structure and function. *Anat Rec* 220:337–356

2. Culav EM, Clark CH, Merrilees MJ (1999) Connective tissues: matrix composition and its relevance to physical therapy. *Phys Ther* 79:308–319
3. Schollmeier G, Lahr-Eigen R, Lewandrowski KU (2000) Observations on fiber-forming collagens in the anulus fibrosus. *Spine (Phila Pa 1976)* 25:2736–2741
4. Antoniou J, Goudsouzian NM, Heathfield TF, Winterbottom N, Steffen T, Poole AR (1996) The human lumbar endplate. Evidence of changes in biosynthesis and denaturation of the extracellular matrix with growth, maturation, aging, and degeneration. *Spine (Phila Pa 1976)* 21:1153–1161
5. Wognum S, Huyghe JM, Baaijens FP (2006) Influence of osmotic pressure changes on the opening of existing cracks in 2 intervertebral disc models. *Spine* 31:1783–1788
6. Drazin D, Rosner J, Avalos P, Acosta F (2012) Stem cell therapy for degenerative disc disease. *Adv Orthop* 2012:961052
7. Raj PP (2008) Intervertebral disc: anatomy-physiology-pathophysiology-treatment. *Pain Practice* 8:18–44
8. Goupille P, Jayson MI, Valat JP, Freemont AJ (1998) Matrix metalloproteinases: the clue to intervertebral disc degeneration? *Spine (Phila Pa 1976)* 23:1612–1626
9. Antoniou J, Steffen T, Nelson F, Winterbottom N, Hollander AP, Poole RA (1996) The human lumbar intervertebral disc: evidence for changes in the biosynthesis and denaturation of the extracellular matrix with growth, maturation, ageing, and degeneration. *J Clin Invest* 98:996–1003
10. Pountos I, Giannoudis PV (2005) Biology of mesenchymal stem cells. *Injury* 36(Suppl 3):S8–S12
11. da Silva MR, Domingues CJ, Pinto RP, Neves N, Matos RM, Tulha JM (2009) New perspectives on degenerative disease treatment. *Acta Reumatol Port* 34:327–335
12. Satomura K, Krebsbach P, Bianco P, Gehron Robey P (2000) Osteogenic imprinting upstream of marrow stromal cell differentiation. *J Cell Biochem* 78:391–403
13. Charbord P, Livne E, Gross G, Haupl T, Neves NM, Marie P (2011) Human bone marrow mesenchymal stem cells: a systematic reappraisal via the genostem experience. *Stem Cell Rev* 7:32–42
14. Risbud MV, Guttapalli A, Tsai TT, Lee JY, Danielson KG, Vaccaro AR (2007) Evidence for skeletal progenitor cells in the degenerate human intervertebral disc. *Spine (Phila Pa 1976)* 32:2537–2544
15. Blanco JF, Graciani IF, Sanchez-Guijo FM, Muntion S, Hernandez-Campo P, Santamaria C (2010) Isolation and characterization of mesenchymal stromal cells from human degenerated nucleus pulposus: comparison with bone marrow mesenchymal stromal cells from the same subjects. *Spine (Phila Pa 1976)* 35:2259–2265
16. Feng G, Yang X, Shang H, Marks IW, Shen FH, Katz A (2010) Multipotential differentiation of human anulus fibrosus cells: an in vitro study. *J Bone Joint Surg Am* 92:675–685
17. Huang B, Liu LT, Li CQ, Zhuang Y, Luo G, Hu SY (2012) Study to determine the presence of progenitor cells in the degenerated human cartilage endplates. *Eur Spine J* 21:613–622
18. Liu LT, Huang B, Li CQ, Zhuang Y, Wang J, Zhou Y (2011) Characteristics of stem cells derived from the degenerated human intervertebral disc cartilage endplate. *PLoS One* 6:e26285
19. Henriksson H, Thornemo M, Karlsson C, Hagg O, Junevik K, Lindahl A (2009) Identification of cell proliferation zones, progenitor cells and a potential stem cell niche in the intervertebral disc region: a study in four species. *Spine (Phila Pa 1976)* 34:2278–2287
20. Brisby H, Papadimitriou N, Brantsing C, Bergh P, Lindahl A, Barreto Henriksson H (2013) The presence of local mesenchymal progenitor cells in human degenerated intervertebral discs and possibilities to influence these in vitro: a descriptive study in humans. *Stem Cells Dev* 22:804–814
21. Turner S, Balain B, Caterson B, Morgan C, Roberts S (2014) Viability, growth kinetics and stem cell markers of single and clustered cells in human intervertebral discs: implications for regenerative therapies. *Eur Spine J* 23:2462–2472
22. Bilic G, Zeisberger SM, Mallik AS, Zimmermann R, Zisch AH (2008) Comparative characterization of cultured human term amnion epithelial and mesenchymal stromal cells for application in cell therapy. *Cell Transpl* 17:955–968
23. Lubis AM, Sandhow L, Lubis VK, Noor A, Gumay F, Merlina M (2011) Isolation and cultivation of mesenchymal stem cells from iliac crest bone marrow for further cartilage defect management. *Acta Med Indones* 43:178–184
24. Thornemo M, Tallheden T, Sjogren Jansson E, Larsson A, Lovstedt K, Nannmark U (2005) Clonal populations of chondrocytes with progenitor properties identified within human articular cartilage. *Cells Tissues Organs* 180:141–150
25. Mochizuki T, Muneta T, Sakaguchi Y, Nimura A, Yokoyama A, Koga H (2006) Higher chondrogenic potential of fibrous synovium- and adipose synovium-derived cells compared with subcutaneous fat-derived cells: distinguishing properties of mesenchymal stem cells in humans. *Arthritis Rheum* 54:843–853
26. Jackson WM, Aragon AB, Bulken-Hoover JD, Nesti LJ, Tuan RS (2009) Putative heterotopic ossification progenitor cells derived from traumatized muscle. *J Orthop Res* 27:1645–1651
27. Hattori S, Oxford C, Reddi AH (2007) Identification of superficial zone articular chondrocyte stem/progenitor cells. *Biochem Biophys Res Commun* 358:99–103
28. Pittenger MF, Mackay AM, Beck SC, Jaiswal RK, Douglas R, Mosca JD (1999) Multilineage potential of adult human mesenchymal stem cells. *Science* 284:143–147
29. Livak KJ, Schmittgen TD (2001) Analysis of relative gene expression data using real-time quantitative PCR and the 2(-Delta Delta C(T)) method. *Methods* 25:402–408
30. Minogue BM, Richardson SM, Zeef LA, Freemont AJ, Hoyland JA (2010) Characterization of the human nucleus pulposus cell phenotype and evaluation of novel marker gene expression to define adult stem cell differentiation. *Arthritis Rheum* 62:3695–3705
31. Minogue BM, Richardson SM, Zeef LA, Freemont AJ, Hoyland JA (2010) Transcriptional profiling of bovine intervertebral disc cells: implications for identification of normal and degenerate human intervertebral disc cell phenotypes. *Arthritis Res Ther* 12:R22
32. Kim YJ, Sah RL, Doong JY, Grodzinsky AJ (1988) Fluorometric assay of DNA in cartilage explants using Hoechst 33258. *Anal Biochem* 174:168–176
33. Enobakhare BO, Bader DL, Lee DA (1996) Quantification of sulfated glycosaminoglycans in chondrocyte/alginate cultures, by use of 1,9-dimethylmethylene blue. *Anal Biochem* 243:189–191
34. Haudenschild DR, McPherson JM, Tubo R, Binette F (2001) Differential expression of multiple genes during articular chondrocyte redifferentiation. *Anat Rec* 263:91–98
35. Dominici M, Le Blanc K, Mueller I, Slaper-Cortenbach I, Marini F, Krause D (2006) Minimal criteria for defining multipotent mesenchymal stromal cells. The International Society for Cellular Therapy position statement. *Cytotherapy* 8:315–317
36. Conley BA, Koleva R, Smith JD, Kacer D, Zhang D, Bernabeu C (2004) Endoglin controls cell migration and composition of focal adhesions: function of the cytosolic domain. *J Biol Chem* 279:27440–27449
37. Musina RA, Bekchanova ES, Sukhikh GT (2005) Comparison of mesenchymal stem cells obtained from different human tissues. *Bull Exp Biol Med* 139:504–509

38. Sakaguchi Y, Sekiya I, Yagishita K, Muneta T (2005) Comparison of human stem cells derived from various mesenchymal tissues: superiority of synovium as a cell source. *Arthritis Rheum* 52:2521–2529
39. Sekiya I, Vuoristo JT, Larson BL, Prockop DJ (2002) In vitro cartilage formation by human adult stem cells from bone marrow stroma defines the sequence of cellular and molecular events during chondrogenesis. *Proc Natl Acad Sci U S A* 99:4397–4402
40. Wilson M, Koopman P (2002) Matching SOX: partner proteins and co-factors of the SOX family of transcriptional regulators. *Curr Opin Genet Dev* 12:441–446
41. Lefebvre V, Huang W, Harley VR, Goodfellow PN, de Crombrughe B (1997) SOX9 is a potent activator of the chondrocyte-specific enhancer of the pro alpha1 (II) collagen gene. *Mol Cell Biol* 17:2336–2346
42. de Crombrughe B, Lefebvre V, Behringer RR, Bi W, Murakami S, Huang W (2000) Transcriptional mechanisms of chondrocyte differentiation. *Matrix Biol* 19:389–394
43. Wang H, Zhou Y, Huang B, Liu LT, Liu MH, Wang J (2014) Utilization of stem cells in alginate for nucleus pulposus tissue engineering. *Tissue Eng Part A* 20:908–920
44. Dawson E, Bernbeck J (1998) The surgical treatment of low back pain. *Phys Med Rehabil Clin N Am* 9:489–495
45. De Ugarte DA, Morizono K, Elbarbary A, Alfonso Z, Zuk PA, Zhu M (2003) Comparison of multi-lineage cells from human adipose tissue and bone marrow. *Cells Tissues Organs* 174:101–109